

**Ribosome heterogeneity results in leader sequence-mediated regulation of
protein synthesis in *Francisella tularensis***

Hannah S. Trautmann¹, Sierra S. Schmidt¹, Steven T. Gregory¹, and Kathryn M. Ramsey^{1,2,*}

¹Department of Cell and Molecular Biology, University of Rhode Island, Kingston, RI 02881, USA

²Department of Biomedical and Pharmaceutical Sciences, University of Rhode Island, Kingston, RI
02881, USA

* To whom correspondence should be addressed: Kathryn M. Ramsey kramsey@uri.edu

Abstract

Although ribosomes are generally examined in aggregate, ribosomes can be heterogenous in composition. Evidence is accumulating that changes in ribosome composition may result in altered function, such that ribosome heterogeneity may provide a mechanism to regulate protein synthesis. Ribosome heterogeneity in the human pathogen *Francisella tularensis* results from incorporation of one of three homologs of bS21, a small ribosomal subunit protein demonstrated to regulate protein synthesis in other bacteria. Loss of one homolog, bS21-2, results in genome-wide post-transcriptional changes in protein abundance. This suggests that bS21-2 can, either directly or indirectly, lead to preferential translation of particular mRNAs. Here, we examine the potential for bS21-2 to function indirectly (via Hfq) and in a leader sequence-dependent manner. While loss of bS21-2 leads to increased abundance of the RNA chaperone Hfq and both Hfq and bS21-2 impact expression of key virulence genes, these proteins influence gene expression via distinct mechanisms. In contrast, we found that the 5' untranslated region (UTR) of some bS21-2 responsive genes, including key virulence genes, is sufficient to alter translation in cells lacking bS21-2. We further identify features of a 5' UTR that allow responsiveness to bS21-2. These include an imperfect Shine-Dalgarno sequence and a particular 6-nucleotide sequence. Our results are consistent with a model in which a bS21 homolog increases efficiency of translation initiation through interactions with specific leader sequences. Together, we determined that ribosome composition in *F. tularensis* regulates translation in a leader sequence-dependent manner, a regulatory mechanism which may be used in other bacteria.

Importance

23 Ribosome heterogeneity is common in bacteria and there is mounting evidence that
24 ribosome composition plays a regulatory role in protein synthesis. However, mechanisms of
25 ribosome-driven gene regulation are not well understood. In the human pathogen *Francisella*
26 *tularensis*, which encodes multiple homologs for the ribosomal protein bS21, loss of one
27 homolog impacts protein synthesis and virulence. Here, we explore the mechanism behind
28 bS21-mediated reductions in protein synthesis, finding that these changes can be linked to
29 altered translation initiation and is dependent on specific sequences in the leaders of transcripts.
30 Our data support a model in which ribosome composition regulates gene expression through
31 translation, a strategy that may be conserved in diverse organisms with various sources of
32 ribosome heterogeneity.

33 Introduction

34 Ribosomes, the molecular machines that synthesize proteins, can be heterogeneous in
35 composition (Genuth & Barna, 2018). As bacterial ribosomes are composed of 3 ribosomal RNA
36 molecules (rRNAs) and ~ 50 ribosomal proteins (r-proteins), heterogeneity can arise from
37 differences in rRNA sequence among *rrn* operons, rRNA or r-protein modification, or r-protein
38 content (Byrgazov et al., 2013). The consequences of ribosome heterogeneity are incompletely
39 understood, and much debate surrounds the hypothesis that distinct classes of ribosomes can
40 have specialized functions by preferentially translating subsets of mRNA (Ferretti & Karbstein,
41 2019).

42 In *E. coli*, the 30S subunit r-protein bS21 is not required for translation *in vitro* but is
43 essential for viability (Bubunencko et al., 2007). It is one of the last proteins to be incorporated
44 during 30S subunit assembly (Mizushima & Nomura, 1970). While the precise function of bS21
45 in translation is not clear, early studies demonstrated its involvement in translation initiation (Held
46 et al., 1974; Chang & Craven, 1977; van Duin & Wijnands, 1981). Association of bS21 with the
47 30S subunit is reversible, as it is easily exchanged among ribosomes (Robertson et al., 1977;
48 Shimojo et al., 2020) suggesting that the presence or absence of bS21 can act as a source of
49 ribosomal heterogeneity.

50 More recently, multiple studies have suggested that bS21 might play a regulatory role in
51 gene expression (Mizuno et al., 2019; Jha et al., 2020; Chen et al., 2022; Trautmann & Ramsey,
52 2022). High-resolution ribosome structures have shown bS21 to be located in the 30S subunit
53 platform, near the mRNA exit channel, and in position to interact with the anti-Shine-Dalgarno
54 (ASD) sequence of 16S rRNA in the 30S initiation complex (Kaledhonkar et al., 2019) and with

55 the Shine-Dalgarno/anti-Shine-Dalgarno (SD-ASD) helix the 70S ribosome (Watson et al.,
56 2020), suggesting possible mechanisms for regulation.

57 Recent work in the Bacteroidia species *Flavobacterium johnsoniae* clearly demonstrates
58 that bS21 controls gene expression. In this organism, incorporation of the single bS21 homolog
59 into the ribosome contributes to sequestration of the ASD (Jha et al., 2020). The mRNA encoding
60 bS21, *rpsU*, is essentially the only *F. johnsoniae* mRNAs with a strong SD sequence. Depletion
61 of bS21 or removal of the region of bS21 necessary for ASD sequestration results in increased
62 translation from the *rpsU* mRNA and mRNAs engineered to have a strong SD (McNutt et al.,
63 2023). These studies unambiguously demonstrate that ribosomes lacking bS21 have altered
64 specificity for particular mRNAs in translation initiation, providing evidence that bS21 functions
65 as a bona fide regulator of gene expression (McNutt et al, 2023).

66 *Francisella tularensis*, a human pathogen that requires a type VI secretion system (T6SS)
67 to cause disease, encodes three distinct homologs of bS21. We have shown that all three
68 homologs can be incorporated into ribosomes. Accordingly, in *F. tularensis*, ribosome
69 heterogeneity may be due to the identity of the bS21 homolog incorporated or, as in *F.*
70 *johnsoniae*, the presence or absence of bS21 in the ribosome. Importantly, loss of one of the
71 homologs, bS21-2, leads to reductions in most T6SS proteins that cannot be explained by
72 changes in transcript abundance or protein stability. Loss of bS21-2 also results in defective
73 intramacrophage replication in cells that can be complemented by restoration of bS21-2, but not
74 by either of the other two homologs. These results indicate that bS21-2 specifically governs
75 translation of virulence genes, including those that encode the T6SS (Trautmann & Ramsey,
76 2022).

77 While our observations support a model in which bS21 proteins in *F. tularensis* regulate
78 gene expression at the level of translation, they are not likely to exert their effects in the same
79 manner as the bS21 homologs in Bacteroidia. In *F. johnsoniae*, the C-terminal region of the
80 single bS21 homolog is required to interact with and sequester the ASD; while this region is
81 conserved amongst the Bacteroidia it is not conserved among other bacterial lineages, including
82 in Gammaproteobacteria like *F. tularensis* (Jha et al., 2020). Thus, in the current study we aim
83 to understand the mechanisms by which bS21-2 affects translation in *F. tularensis*.

84 Using qPCR and immunoblot analyses, we show that bS21-2 and the RNA-binding
85 protein Hfq both govern T6SS protein abundance but do not act in a coordinated manner and
86 function via distinct pathways. Through reporter assays using translational fusions, we see that
87 the 5' untranslated region (5' UTR) of some transcripts is sufficient to cause differences in
88 protein production if bS21-2 is lost, indicating that these 5' UTRs are responsive to bS21-2. By
89 mutagenizing the bS21-2-responsive 5' UTRs, we also found that transcripts with ideal SD
90 sequences do not require bS21-2 for efficient translation. In an attempt to identify which
91 component of the 5' UTR is driving the responsiveness to bS21-2, we determined that the
92 secondary structure of the leader sequence does not play a clear role and that two motifs
93 enriched in bS21-2-controlled genes are not needed to cause changes in protein abundance.
94 Finally, we identified a short nucleotide sequence in the 5' UTR of *mraY* that is critical for control
95 by bS21-2. Our findings suggest that the r-protein bS21-2 governs protein abundance in *F.*
96 *tularensis* by influencing translation from mRNA species with specific leader sequences.

97

98 Results

99 ***bS21-2 and Hfq influence T6SS protein abundance via different mechanisms***

100 While the small subunit ribosomal protein bS21-2 post-transcriptionally governs the
101 abundance of many genes, including those that encode T6SS proteins essential for
102 intramacrophage growth, the mechanism by which this occurs is unknown (Trautmann &
103 Ramsey, 2022). In considering the control of the T6SS proteins, we first hypothesized that bS21-
104 2 may be exerting its effects indirectly, by modifying the abundance of a regulator that directly
105 controls production of the T6SS proteins. One such candidate is the RNA-binding protein Hfq,
106 which is known to control gene expression post-transcriptionally in many organisms and has
107 been shown to impact the expression of T6SS proteins in *F. tularensis* (Meibom et al., 2009;
108 Lenco et al., 2014). Our proteomics analysis identified increased Hfq in cells lacking bS21-2
109 compared to wild-type (5.9-fold), although substantial variation in biological replicates precluded
110 the differences from reaching statistical significance (adj p=0.066; Trautmann & Ramsey, 2022).
111 Additionally, many of the genes impacted by bS21-2 have AU-rich 5' UTRs that resemble ARN-
112 motifs, known targets of Hfq (Link et al., 2009). This led us to hypothesize that Hfq may play a
113 role in bS21-2-mediated regulation of T6SS proteins.

114 To test further whether cells lacking bS21-2 have increased Hfq, we added DNA
115 specifying a C-terminal vesicular stomatitis virus glycoprotein (VSV-G) epitope tag to *hfq* in cells
116 with (WT) and without ($\Delta rpsU2$) bS21-2 and determined relative protein abundance by
117 quantitative immunoblotting. We found a moderate increase in Hfq (about 30%, **Fig 1A**) in cells
118 lacking bS21-2 compared to wild-type; this is consistent with our prior proteomics findings,
119 including that it is not a difference that would have reached our significance threshold.

120 Given the detectable increase in Hfq abundance in cells lacking bS21-2, we sought to
121 determine if this is due to increased translation of the *hfq* mRNA. Using a reporter assay with a
122 GFP translational fusion (described in more detail below), we assessed the relative translation
123 of mRNAs containing the *hfq* 5' UTR. Briefly, reporters expressing either the 5' UTR of *hfq* or a
124 control 5' UTR (*tul4*) fused to *gfp* were introduced into cells with and without bS21-2. We found
125 that there is approximately 2-fold more GFP produced from reporter fusions with the 5' UTR of
126 *hfq* in cells lacking bS21-2, indicating this UTR leads to more efficient translation by ribosomes
127 without bS21-2 (**Fig 1B**). This suggests that the observed increase in Hfq in cells lacking bS21-
128 2 is due to increased translation initiation.

129 If the moderate increase in Hfq leads to the observed reduction in T6SS proteins when
130 bS21-2 is absent, Hfq must be acting as a repressor of the T6SS. However, inconsistent results
131 have been reported with respect to the role of Hfq in regulating the T6SS genes in *F. tularensis*.
132 A transcriptomic analysis of cells lacking Hfq found that one of the two Francisella Pathogenicity
133 Island (FPI) operons encoding the T6SS, the *pdpA* operon, was upregulated in *hfq* mutant cells
134 (Meibom et al., 2009). In another report, a proteomic analysis of *hfq* mutant cells found that
135 proteins encoded by the other FPI operon, the *iglA* operon, are less abundant but observed no
136 change in the abundance of proteins encoded by the *pdpA* operon (Lenco et al., 2014). To clarify
137 the role of Hfq in the regulation of T6SS protein abundance, we determined the abundance of
138 several T6SS proteins encoded on both FPI operons in cells with and without Hfq by quantitative
139 immunoblotting (**Fig 1C**) (Trautmann & Ramsey, 2022). PdpB, encoded in the *pdpA* operon, was
140 more abundant in cells without Hfq compared to wild-type (>2-fold; $p < 0.01$), while IgIB and IgIA,
141 encoded on the *iglA* operon, were not impacted by the loss of Hfq (**Fig 1C**). This is in contrast
142 to cells lacking bS21-2, which contained reduced amounts of all three proteins (**Fig 1C**;

143 Trautmann & Ramsey, 2022). These data suggest that Hfq regulates expression of proteins
144 encoded by the *pdpA* operon, but not the *iglA* operon, consistent with the observations of
145 Meibom et al. (2009).

146 Hfq can exert its effects through a variety of mechanisms, some of which result in changes
147 in translation initiation. To determine if the presence of *F. tularensis* Hfq, like bS21-2, impacts
148 the translation of T6SS proteins, we analyzed the ability of cells lacking Hfq to translate mRNAs
149 containing either the 5' UTRs of the T6SS protein gene *pdpA* or the control gene *tul4* fused to
150 *gfp*. We found that translation of mRNAs with the *pdpA* or *tul4* 5' UTRs are not altered when Hfq
151 is absent compared to wild-type, while translation of the mRNA with the *pdpA* 5' UTR decreases
152 if bS21-2 is absent (**Fig 1D**). These findings suggest that while bS21-2-associated changes in
153 T6SS proteins can be attributed to changes in translation initiation, Hfq-associated changes in
154 T6SS proteins cannot.

155 Since it has been proposed that Hfq represses *pdpA* operon transcript abundance
156 (Meibom et al., 2009) and Hfq does not impact translation of *pdpA* in a 5' UTR-dependent
157 manner, we hypothesized that cells lacking Hfq might have increased PdpB due to increased
158 *pdpB* (and *pdpA* operon) transcript abundance. To test this, we compared the abundance of
159 mRNAs isolated from wild-type cells to those isolated from cells lacking bS21-2 ($\Delta rpsU2$) or Hfq
160 (Δhfq) by qPCR, and found that *pdpA* and *pdpB* transcripts have large, statistically significant
161 increases when Hfq is not present (42-fold and 69-fold, respectively) but the relative impact on
162 *iglA* transcript abundance is minor (2.5-fold increased) (**Fig 1E**); this is in contrast to the minor
163 changes in *pdpA*, *pdpB*, and *iglA* transcripts in cells without bS21-2 (~2-fold or less).

164 Our findings indicate that Hfq exerts its effects on a subset of T6SS proteins by negatively
165 regulating their transcript abundance (**Fig 1E**). Conversely, bS21-2 influences the abundance of
166 essentially all the T6SS proteins and does so by influencing their protein synthesis rather than
167 their transcript abundance (**Fig 1D** and Trautmann & Ramsey, 2022). Given that Hfq and bS21-
168 2 influence distinct groups of proteins at different points in gene expression, our work does not
169 support a model in which Hfq mediates the effects of bS21-2 on the T6SS. Instead, our results
170 suggest two distinct pathways of regulation for the genes encoding the T6SS: one in which bS21-
171 2 improves efficiency of translation initiation from both operons, and one in which Hfq represses
172 transcript abundance of only the *pdpA* operon.

173 ***bS21-2 promotes translation of specific genes in a 5' UTR-dependent manner***

174 In *E. coli*, bS21 has been implicated in sequence-dependent translation initiation and, in
175 the ribosome, is located adjacent to the 5' untranslated region (UTR) of mRNAs during
176 translation initiation (Kaledhonkar et al., 2019; van Duin & Wijnands, 1981). Loss of bS21-2 in
177 *F. tularensis* leads to changes in abundance for a subset of the proteome (Trautmann & Ramsey,
178 2022). This led us to hypothesize that bS21-2 may directly impact protein abundance by
179 modulating translation initiation in a 5' UTR-dependent manner. In order to test this hypothesis,
180 our goal was to assess the role of 5' UTR sequences in bS21-2-mediated translation of particular
181 genes. To accomplish this, we developed a series of reporter constructs consisting of the
182 experimentally determined or predicted 5' UTR with the first 6 codons of the gene of interest,
183 fused to a reporter gene (*lacZ* or *gfp*) (**Fig 2A**; also as in **Fig 1B** and **1D**). Reporter constructs
184 were expressed from the *tul4* promoter, which is unaffected by the presence or absence of bS21-
185 2 (Trautmann & Ramsey, 2022). This design allows for comparable transcription of reporter

186 genes in both genotypes to compare relative translation initiation. The reporter constructs were
187 introduced into either wild-type *F. tularensis* (WT) or *F. tularensis* lacking bS21-2 ($\Delta rpsU2$).
188 Some experiments were completed using β -galactosidase reporters incorporated into the
189 chromosome at the Tn7 site. Toxicity of plasmids that produce high levels of β -galactosidase in
190 *E. coli* during plasmid production led us to use a GFP-based reporter system for some
191 constructs. Reporter constructs using *gfp* were cloned into a multi-copy plasmid that is retained
192 at essentially the same copy number in *F. tularensis* cells with and without bS21-2 (**Fig S1**).

193 These reporter assays evaluated the relative efficiency of translation initiation of specific
194 5' UTRs in cells with or without bS21-2. We chose to assess the 5' UTRs corresponding to
195 genes with significant changes in protein abundance in cells lacking bS21-2 (Trautmann &
196 Ramsey, 2022). Consistent with the observed changes in protein abundance being due to
197 changes in translation initiation, we found that the 5' UTRs of *pdpA*, *iglA*, *mraY*, FTL_0222, or
198 FTL_1093 genes fused to *gfp* led to significantly less fluorescence in cells lacking bS21-2
199 compared to wild-type (**Fig 2B**). In contrast, the 5' UTR of *tul4*, a gene not differentially
200 expressed in cells lacking bS21-2, did not lead to a significant decrease in fluorescence in cells
201 lacking bS21-2 (**Fig 2B**). These data reveal that the 5' UTR of a gene is sufficient for bS21-2 to
202 affect translation and is consistent with the idea that bS21 may be regulating translation initiation.
203 We will refer to 5' UTRs that result in altered protein abundance in the presence of bS21-2 as
204 "bS21-2-responsive." We also found that the 5' UTRs of some genes governed by bS21-2 in our
205 proteomics analysis did not lead to reporter gene differences in cells lacking bS21-2, including
206 FTL_0881 and FTL_0215 (**Fig S2**). We do not have experimentally determined transcription
207 start sites for these genes, so it is possible the lack of regulation is due to inaccurate 5' UTR
208 predictions. Other possibilities, including indirect regulation of these particular genes, are

209 described in the discussion. We confirmed that alterations in protein production in cells lacking
210 bS21-2 could be complemented by ectopic expression of bS21-2 from a plasmid, indicating that
211 the changes in translation are not due to polar effects of the *rpsU2* deletion (**Fig S3**).

212 ***An ideal Shine-Dalgarno sequence masks the positive effects of bS21-2 on translation***

213 Given that the FPI gene *pdpA* has a bS21-2-responsive 5' UTR (**Fig 1D and 2A**), we
214 further examined features of the *pdpA* 5' UTR that may lead to preferential translation from
215 ribosomes containing bS21-2. Based on structures of the *E. coli* ribosome during translation
216 initiation, the bS21 residue R17 is close enough to directly contact the 16S rRNA nucleotide
217 C1529, which is part of the anti-Shine Dalgarno sequence (Kaledhonkar et al., 2019; **Fig 3A**).
218 R17 is conserved in all three *F. tularensis* bS21 homologs and the rRNA-encoded ASD is
219 identical in *F. tularensis* and *E. coli*. Thus, we hypothesized that bS21 homologs in *F. tularensis*
220 may also contact the ASD and influence SD binding during translation initiation. To test this
221 possibility, we developed β -galactosidase translational reporters with altered SD sequences in
222 the *pdpA* 5' UTR (**Fig 3B**). 5' UTRs with mutations that retained imperfect base-pairing between
223 the ASD and SD (badSD, *tul4SD*) were still bS21-2-responsive. However, introducing an ideal
224 SD, in two different positions (idealSD, ideal_movedSD), led to similar reporter gene expression
225 in cells with and without bS21-2, indicating that these 5' UTRs are no longer bS21-2-responsive
226 (**Fig 3B**).

227 We replicated the impact of a perfect SD on the bS21-2 responsive 5' UTR of another
228 gene, *mraY*. Modification of the imperfect *mraY* SD to an ideal SD resulted in no significant
229 difference in GFP production in cells with or without bS21-2 (**Fig 3C**). It is worth noting that in
230 each of these cases, the addition of a perfect SD in the correct location (separated from the start

231 codon by 6 to 8 nt) leads to increased total reporter production (**Fig S4**). These data suggest
232 that genes with perfect SD sequences do not require bS21-2 for efficient translation; in other
233 words, an ideal SD may lead to such efficient translation that any response to bS21-2 becomes
234 negligible.

235 Because perfect SD sequences mask the impacts of bS21-2, we hypothesized that genes
236 with weaker SD sequences may require bS21-2 for efficient translation. We compared predicted
237 SDs for genes whose proteins are positively affected (n=74), negatively affected (n=84), or
238 unaffected (n=82) by bS21-2 (Trautmann & Ramsey, 2022). We found that the genes positively
239 affected by bS21-2 generally have weaker SD sequences, with only 39% having strong SD
240 sequences (defined by 4 or more nucleotides [nt] complementary to the ASD), compared to 54%
241 or 69% strong SDs in negatively affected or unaffected genes, respectively (**Fig 3D**). These data
242 are consistent with a model in which bS21-2 influences translation initiation predominately in the
243 absence of strong SD-ASD interactions. However, given that many *F. tularensis* genes have
244 weak or non-perfect SDs and are not affected by bS21-2, there is an unidentified component of
245 the 5' UTR that results in responsiveness to bS21-2.

246 ***Sequence-specific motifs found in the 5' UTR of genes governed by bS21-2 do not alter***
247 ***bS21-2 responsiveness***

248 We reasoned that 5' UTRs may be responsive to bS21-2 because they harbor a common
249 sequence-specific element that mediates an altered interaction with bS21-2 or bS21-2-
250 containing ribosomes. To identify such an element, we compiled 5' UTR sequences including
251 100 nts upstream of the start codon and the first six codons of the gene for all proteins that were
252 significantly less abundant in cells lacking bS21-2 compared to wild-type (n=74; 100 nt was

253 arbitrarily chosen because most *F. tularensis* transcription start sites have not been identified).
254 As a control, we also compiled 5' UTR sequences from 82 genes that were not impacted by
255 bS21-2 presence. Using the motif-finding algorithm STREME, which identifies ungapped motifs
256 enriched in large data sets (Bailey, 2021), we identified sequence motifs enriched in the 5' UTRs
257 of the 20 genes most positively governed by bS21-2 (Trautmann & Ramsey, 2022). The motifs
258 we identified were enriched compared to shuffled sequences and were not found to be enriched
259 in the control sequences. Two motifs, which we refer to as Motif 1 and Motif 2, are AU-rich and
260 are found in 19 and 18 of the 20 sequences assessed, respectively (**Fig 4A**). Targeted mutations
261 were made to modify these motifs in the *mraY* 5' UTR and assess their impact on
262 responsiveness to bS21-2. Mutations 1 and 2 modified Motif 1 from AAAUAAC to
263 CCCC GCCG, which altered the AU-content of the entire motif, and AAAUAUACA, which altered
264 the three most conserved nt in the motif. When assessed using the GFP reporter assay, neither
265 of these modifications altered the responsiveness of the 5' UTR to bS21-2 (**Fig 4B**). To assess
266 the contribution of Motif 2, we created mutation 5, a truncation of the 5' end of the *mraY* 5' UTR
267 that removed 25 nt including motif 2. This mutant 5' UTR also remained responsive to bS21-2
268 (**Fig 6**). Together, these data indicate that neither of the two STREME-predicted AU-rich motifs
269 are necessary for the positive impact of bS21-2 on translation of the *mraY* 5' UTR.

270 ***Predicted secondary structures of 5' UTRs are not responsible for bS21-2*** 271 ***responsiveness***

272 The secondary structure of mRNA molecules is an important determinate of translation
273 initiation efficiency (Hall et al., 1982; de Smit & van Duin, 1994). We hypothesized that mRNA
274 secondary structure may play a role in bS21-2-mediated translation. We predicted the secondary

275 structure of the *pdpA* 5' UTR using MXfold2 (**Fig S5**), made targeted mutations to disrupt the
276 predicted stem-loop structure (*pdpA* mut1), and generated β -galactosidase reporters at the Tn7
277 site in cells with (WT) and without ($\Delta rpsU2$) bS21-2 (**Fig 5A**). We also made complementary
278 mutations to restore the original predicted secondary structure without maintaining the original
279 sequence (*pdpA* mut2). In designing each mutation, we ensured that there was no significant
280 disruption to the Shine-Dalgarno or start codon. Neither of these variants that altered the *pdpA*
281 5' UTR structure affected responsiveness to bS21-2, indicating that the secondary structure of
282 this 5' UTR does not play a role in translation modulation by bS21-2.

283 We then looked at the secondary structure of a longer 5' UTR, *mraY*, which was predicted
284 using MXFold2 to contain a large stem-loop (**Fig 5B**). We mutated a region that was predicted
285 to form the stem closest to the loop, thereby disrupting the structure (*mraY* mut3). We also made
286 complementary mutations to restore the structure (*mraY* mut4) and assessed these 5' UTRs in
287 a GFP reporter assay. We found that the disruption to the predicted secondary structure (*mraY*
288 mut3) did not affect bS21-2 responsiveness. In contrast, the complementary mutation that
289 restored the stem-loop structure was no longer responsive to bS21-2 (**Fig 5B**). In our studies of
290 two different bS21-2 responsive 5' UTRs, we did not find a specific predicted secondary structure
291 that is necessary for bS21-2-responsive translation.

292 ***A 6-nucleotide region of the mraY 5' UTR is critical for bS21-2-responsiveness***

293 While testing the importance of the *mraY* 5' UTR structure to bS21-2 responsiveness, we
294 identified a 5' UTR variant that was no longer responsive to bS21-2 (*mraY* mut4). This variant
295 included mutations in nt 58-63 upstream of the initiation codon. To further clarify the sequence
296 necessary for bS21-2-responsiveness in the *mraY* 5' UTR, we made a series of truncations and

297 modifications from the 5' end of the leader sequence. Truncating the 5' UTR to 75 nt (*mraY*
298 mut5) did not impact bS21-2-responsiveness, nor did modifying the AU-rich region located 64-
299 70 nt from the initiation codon (*mraY* mut8) (**Fig 6**). But truncating the 5' UTR to 57 nt (*mraY*
300 mut6) led to loss of bS21-2-responsiveness, further implicating the nt 58-63 upstream of the
301 initiation codon, GACUCU, in responsiveness to bS21-2, as suggested by *mraY* mut4 (**Fig 5B**).
302 We further assessed the importance of the GACUCU sequence using *mraY* mut7 (truncating the
303 5' UTR to 60 nt and changing the first three nt to AGA) and *mraY* mut9 (truncating the 5' UTR
304 to 63 and mutating nt 58-63 to AGUGAG) and found neither was responsive to bS21-2 (**Fig 6**).
305 These data allow us to conclude that the nt 58-63 upstream of the *mraY* initiation codon,
306 GACUCU, are critical for bS21-2-responsive translation of the *mraY* 5' UTR. This is consistent
307 with a model in which bS21-2-containing ribosomes interact directly or indirectly with a specific
308 element of the leader sequence to facilitate efficient translation initiation on some transcripts.

309

310 **Discussion**

311 In this work, we addressed two hypotheses regarding how bS21-2 exerts its effects on
312 protein synthesis. In the first, we suggested that the effects of bS21-2 on the T6SS proteins may
313 be mediated by Hfq, a known regulator of T6SS proteins. However, since there have been
314 conflicting reports regarding the impacts of Hfq on the T6SS, we also examined the effects of
315 Hfq on T6SS protein and transcript abundance. Our work clearly demonstrates that Hfq is a
316 negative regulator of one of the two FPI operons encoding T6SS proteins and that this regulation
317 influences transcript abundance rather than translation, consistent with and building upon, a prior
318 study (Meibom et al., 2009). In contrast, the positive effects of bS21-2 on essentially all T6SS

319 proteins can be attributed to differences in protein synthesis. Thus, we conclude that Hfq and
320 bS21-2 function in independent pathways to regulate the T6SS proteins. The second hypothesis
321 we addressed is that ribosomes containing bS21-2 may influence translation initiation of specific
322 transcripts in a leader sequence-dependent manner. Using reporter assays, we determined that
323 specific 5' UTR sequences are sufficient to lead to altered translation in cells with or without
324 bS21-2. In a comprehensive assessment of 5' UTR elements, we found that bS21-2 responsive
325 5' UTRs have imperfect SD sequences and, in a specific responsive 5' UTR, the presence of a
326 particular six nucleotide sequence. Together, these results suggest that bS21-2 impacts protein
327 synthesis by altering translation initiation on mRNAs with specific leader sequences.

328 In *F. tularensis*, loss of the RNA chaperone Hfq results in defective intramacrophage
329 replication, which is essential for virulence. Yet how Hfq promotes *F. tularensis* intramacrophage
330 replication remains poorly-understood. Few small RNAs have been identified in *F. tularensis* and
331 none have been identified that are Hfq-dependent (Postic et al., 2010; Postic et al., 2012). Two
332 prior studies determined that cells without Hfq have altered expression of the T6SS genes,
333 encoded on the FPI (Meibom et al., 2009; Lenco et al., 2014). One study reported that cells
334 lacking Hfq have increased transcript abundance of only the *pdpA* operon genes, while the other
335 identified decreased abundance of proteins encoded by the *iglA* operon (Meibom et al., 2009;
336 Lenco et al., 2014). Our results are consistent with the former report, that Hfq acts as a negative
337 regulator of *pdpA* operon transcript abundance. We additionally demonstrate a concordant
338 increase in protein abundance for a gene encoded on the *pdpA* operon in cells lacking Hfq.
339 Finally, using a translational reporter fusion, we show that changes in protein abundance for
340 genes in the *pdpA* operon are not due to changes in translation efficiency. These results
341 demonstrate that Hfq acts to repress *pdpA* operon transcript abundance but does not appear to

342 influence T6SS protein synthesis. The molecular mechanism by which Hfq exerts its effects on
343 this operon, and if it involves a small RNA, remain unclear. Regardless, the change in production
344 of T6SS components in cells lacking Hfq is consistent with the observed intramacrophage growth
345 defect, as *F. tularensis* cells overproducing the T6SS are defective for intramacrophage survival
346 (Rohlfing et al., 2018).

347 This work demonstrates that bS21-2 exerts its effects on protein synthesis in a leader
348 sequence-dependent manner and is validated in a subset of bS21-2-responsive 5' UTRs (**Fig**
349 **2**). While loss of bS21-2 results in altered abundance for about 160 proteins (Trautmann &
350 Ramsey, 2022), we expect that changes in protein abundance for at least some of these may
351 not be due to leader sequence-dependent effects, but rather due to downstream or secondary
352 effects. For example, bS21-2 may directly impact synthesis of proteins that influence the
353 abundance of other proteins. Several proteases and peptidases were found to be differentially
354 abundant in cells lacking bS21-2. Thus, proteins like those encoded by FTL_0881 and FTL_0215
355 may have altered abundance in bS21-2 mutant cells due to changes in the abundance of
356 proteases or protein processing genes.

357 In our search for an element responsible for leader sequences to be responsive to bS21-
358 2, we found that ideal SD sequences prevent responsiveness. Additionally, leader sequences
359 with perfect SDs result in much higher translation (**Fig S4**). This suggests that perfect SD-ASD
360 complementarity leads to such efficient translation initiation that any contribution of bS21-2 to
361 translation are minor and effectively masked. It is perhaps unsurprising that other regulators of
362 translation, such as H-NS in *E. coli*, similarly function to regulate translation of mRNAs with
363 imperfect SDs (Park et al., 2010).

364 While we were unsuccessful at identifying a common element across all bS21-2
365 responsive leader sequences, we were able to hone in on the 6 nt sequence in the *mraY* 5' UTR
366 that leads to bS21-2 responsiveness, GACUCU. It is notable that this 6 nt sequence, which is
367 found 58-63 nt away from the initiation codon, is predicted to form a stem-loop via
368 complementary base-pairing to a sequence 3 nt away from the SD. Yet disruption of the
369 predicted structure by mutating the complementary sequence does not impact the response to
370 bS21-2, implicating the distant 6 nt sequence alone. We speculate that the 6 nt GACUCU
371 sequence may be a direct binding site for bS21-2, and that a direct interaction between this site
372 and bS21-2 in the ribosome increases translation initiation of the *mraY* mRNA. However, this
373 specific sequence is not found in other bS21-2 responsive leader sequences (including the short,
374 24 nt *pdpA* 5' UTR). Further work will be necessary to determine if this sequence is sufficient for
375 bS21-2 responsiveness, to identify the commonalities among bS21-2 responsive 5' UTRs, and
376 to determine how bS21-2 influences translation initiation on specific leader sequences.

377 **Materials and Methods**

378 ***Bacterial strains and growth conditions***

379 Unless otherwise noted, bacterial strains were grown as indicated. *Francisella tularensis*
380 subsp. *holarctica* Live Vaccine Strain (LVS) cells were grown in Mueller-Hinton broth (BD Difco)
381 supplemented with 0.025% iron pyrophosphate, 0.1% glucose, and 2% Isovitalex (sMHB),
382 shaking aerobically or on cystine heart agar (BD Difco or prepared in house) plates with 1%
383 hemoglobin (CHA-H) at 37°C. *Escherichia coli* XL1-Blue, DH5α (New England Biolabs), and
384 DH5α λ-pir cells were grown in lysogeny broth (LB) shaking aerobically or on LB agar plates at
385 37°C. Kanamycin and nourseothricin were used at concentrations of 5 µg/mL (*F. tularensis*) or
386 50 µg/mL (*E. coli*); hygromycin B was used at concentrations of 200 µg/mL. *Saccharomyces*
387 *cerevisiae* cells were grown in synthetic defined (SD) broth without uracil (-ura) shaking
388 aerobically or on SD-ura agar plates at 30°C.

389 ***Vector construction***

390 Tn7::lacZ plasmids

391 Mini-Tn7 plasmids for each β-galactosidase reporter were created from a plasmid derived
392 from pMP749 (LoVullo et al., 2009). *E. coli lacZ* was amplified from pEX-pigR::lacZ (Charity et
393 al., 2009) using a 5′ primer specifying a NotI site and alanine linker (5′-GCGGCCGCT-3′) and
394 a 3′ primer specifying a BamHI site. The amplified *lacZ* gene was cloned into NotI/BamHI
395 digested pMP749, resulting in pKR68 (Tn7-lacZ). Subsequently, two fragments were amplified
396 from LVS genomic DNA (gDNA): (1) the *tul4* promoter with a 5′ primer specifying a KpnI site
397 and a 3′ primer overlapping the second fragment; and (2) either modified or wild-type UTRs from
398 genes of interest, along with the first six codons of the corresponding gene, with a 3′ primer

399 specifying a NotI site and a 5' primer overlapping the first fragment. Overlap extension PCR was
400 then conducted on the two fragments and the PCR product was cloned into KpnI/NotI digested
401 pKR68 such that *lacZ* was in-frame with the first six codons of the gene of interest. The resulting
402 plasmids are all indicated in **Supplemental Table 1**. Modifications to wild-type UTRs were
403 encoded on primers for PCR amplification.

404 Some reporter plasmids with the high-copy pUC *ori* produced enough β -galactosidase in
405 *E. coli* to be toxic, so cloning required one of two alternate approaches. In one approach, the
406 origin of the pMP749 plasmid was replaced by a low-copy R6K γ origin, amplified from pKL91
407 (Ramsey et al., 2020) using primers that encode an NspI site. The digested product was cloned
408 into NspI-digested pMP749, resulting in pKR88 (Mini_Tn7_R6Kg)., which was propagated in
409 DH5 α λ -pir cells. Subsequently, the *tul4* promoter and 5' UTR was amplified from LVS gDNA
410 using a 5' primer specifying a KpnI and a 3' primer specifying a NotI site; *lacZ* was amplified
411 from pKR68 using a 5' primer specifying a NotI site and alanine linker (5'-GCGGCCGCT-3')
412 and a 3' primer specifying a BamHI site. The two fragments were cloned into BamHI/KpnI-
413 digested pKR88 using a three-way ligation, resulting in pKR89
414 (Tn7_P*tul4*_tul4UTR_*lacZ*_R6Kg; **Supplemental Table 1**).

415 In a second approach, *lacZ* plasmids were cloned using *Saccharomyces cerevisiae*. The
416 2 μ origin and *URA3* gene were isolated from pYES2 (Invitrogen) by digestion with PstI, then
417 cloned into DraI-digested pKR68, disrupting the β -lactamase gene. The resulting plasmid,
418 pKR128 pYES2 Tn7-*lacZ*, was used for subsequent cloning of 5' UTRs using alanine linkers
419 and NotI sites, as described above and detailed in **Supplemental Table 1**. pYES2-based
420 plasmids were purified from overnight cultures of *S. cerevisiae* using the Zymoprep Yeast
421 Plasmid Miniprep III kit.

422 pF-GFP plasmids

423 Multicopy GFP reporter plasmids were created from a previously described shuttle vector,
424 pFNLTP6 (Maier et al., 2004). A fragment containing the promoter, 5' UTR, and first six codons
425 of *tul4* was digested from pKR89 with KpnI/NotI. sfGFP codon-optimized for expression in *F.*
426 *tularensis* LVS was purchased as a gBlock (IDT) and digested with NotI/BamHI. Fragment were
427 cloned into KpnI/BamHI-digested pF such that GFP was in-frame with the first six codons of *tul4*,
428 resulting in pKR145 (pF-*tul4* UTR-GFP). The plasmid pKR146 (pF-*pdpA* UTR-GFP) was
429 constructed similarly, after amplification from pKR74 of the *tul4* promoter and *pdpA* 5' UTR and
430 first six codons and digestion of the PCR product with Kpn/NotI. Subsequent constructs were
431 cloned into pKR145 to replace the *tul4* 5' UTR using the endogenously encoded PacI site in the
432 *tul4* promoter (**Supplemental Table 1** for details). For genes in which a transcription start site
433 had not been annotated at the time of plasmid design, 100 nucleotides upstream of the start
434 codon were included as the 5' UTR (**Supplemental Table 1** for details). Known transcription
435 start sites for *tul4*, *iglA*, and *pdpA* were previously published by Ramsey et al. (2015); the
436 transcription start site for *hfq* was experimentally determined by Meibom et al. (2009) and
437 Chambers & Bender (2011).

438 pF-nat complementation vector

439 The pF-*rpsU2*-V plasmid (pKR7, Trautmann & Ramsey, 2022) was modified to replace
440 the kanamycin resistance cassette with a nourseothricin (nat) resistance cassette from pF3-
441 MglA-V as previously described (Rohlfing and Dove, 2014), yielding pKR15 pF-nat-*rpsU2*-V.

442 Allelic exchange plasmid

443 The plasmid pEX18kan was modified to create the in-frame deletion construct for deletion
444 of *hfq* as previously described (Charity et al., 2007). Flanking regions of ~1000 base pairs from
445 both sides of the *hfq* gene were amplified by PCR. Primers amplifying the DNA adjacent to *hfq*
446 included the first three or last three codons of the open reading frame and DNA specifying a NotI
447 site, which also encodes an alanine linker (5'-GCGGCCGCT-3'). The two fragments were
448 cloned into BamHI/KpnI-digested pEX18kan, yielding pKL111 pEXΔ*hfq*.

449 VSV-G tagging integration vector

450 A single-integration vector for VSV-G tagging of *hfq* was made by modifying pKL02
451 (Ramsey et al., 2015). The final 200 nucleotides of the 3' end of *hfq* was amplified using a 5'
452 primer specifying a KpnI site and a 3' primer that lacked the native stop codon and included
453 DNA specifying a NotI site. The fragment was cloned into KpnI/NotI digested pKL02 such that
454 the 3' end of *hfq* is in frame with the codons specifying three alanine residues followed by the
455 VSV-G epitope, resulting in pKR158 (pEX-*hfq*-V).

456 **Strain construction**

457 β-galactosidase reporter strains (**Table 1**) were constructed by site- and orientation-
458 specific single chromosome integration using the Tn7 transposon as previously described
459 (LoVullo et al., 2009). Helper plasmid pMP720 was electroporated into either wild-type (LVS) or
460 bS21-2 mutant (Δ*rpsU2*) competent cells in 0.2 cm cuvettes with a 2.5 kV pulse and hygromycin-

461 resistant cells were selected by plating on CHA-H with hygromycin. Cells with the helper plasmid
462 were electroporated with the appropriate mini-Tn7 plasmid and selected for on CHA-H with
463 kanamycin. Colonies were screened for plasmid integration at the *attTn7* site using PCR.
464 Candidate strains were confirmed by amplification of genomic DNA outside of the *attTn7* site
465 and Sanger sequencing.

466 Reporter constructs encoded on pF plasmids were electroporated into LVS, LVS $\Delta rpsU2$,
467 or LVS Δhfq cells as described above and selected for on CHA-H with kanamycin (**Table 1**). The
468 complementation vectors or empty pF plasmids were electroporated into β -galactosidase
469 reporter strains as described above and selected for on CHA-H with nourseothricin.

470 The Hfq deletion strain was constructed by allelic exchange as previously described
471 (Trautmann & Ramsey 2022). Briefly, at least 1 μ g of allelic exchange plasmid pEX Δhfq was
472 electroporated into competent cells as above. Cells in which a single integration event occurred
473 were selected for on CHA-H-kanamycin. Counter-selection for the vector was accomplished by
474 plating on CHA-H (BD Difco) containing 10% sucrose. Sucrose-resistant, kanamycin-sensitive
475 colonies were screened for deletions using PCR. Candidate strains were confirmed by
476 amplification of genomic DNA outside of the flanking regions on each side of the deletion and
477 Sanger sequencing, validating LVS Δhfq .

478 Cells with VSV-G-tagged Hfq were made as previously described (Ramsey et al., 2015).
479 Briefly, at least 1 μ g of pKR158 pEX-*hfq*-V was electroporated into LVS and $\Delta rpsU2$ cells and
480 transformants were selected on CHA-H-with kanamycin. Cells were confirmed to have a single
481 integration by PCR amplification of DNA across the integration site and subsequent Sanger
482 sequencing of the PCR product.

Table 1: Strains used in this study

Strain Number	Description	Genetic Background	Plasmid
β-galactosidase reporter strains			
KRLVS96	LVS Tn7::Ptul4-pdpA 5'UTR-lacZ aphA	LVS	pKR74
KRLVS97	LVS $\Delta rpsU2$ Tn7::Ptul4-pdpA 5'UTR-lacZ aphA	$\Delta rpsU2$	pKR74
KRLVS102	LVS Tn7::Ptul4-pdpA 5'UTR-mut1-lacZ aphA	LVS	pKR84
KRLVS106	LVS $\Delta rpsU2$ Tn7::Ptul4-pdpA 5'UTR-mut1-lacZ aphA	$\Delta rpsU2$	pKR84
KRLVS110	LVS Tn7::Ptul4-pdpA 5'UTR-mut2-lacZ aphA	LVS	pKR85
KRLVS107	LVS $\Delta rpsU2$ Tn7::Ptul4-pdpA 5'UTR-mut2-lacZ aphA	$\Delta rpsU2$	pKR85
KRLVS114	LVS Tn7::Ptul4-pdpA 5'UTR-badSD-lacZ aphA	LVS	pKR98
KRLVS117	LVS $\Delta rpsU2$ Tn7::Ptul4-pdpA 5'UTR-badSD-lacZ aphA	$\Delta rpsU2$	pKR98
KRLVS115	LVS Tn7::Ptul4-pdpA 5'UTR-ideal movedSD-lacZ aphA	LVS	pKR99
KRLVS118	LVS $\Delta rpsU2$ Tn7::Ptul4-pdpA 5'UTR-ideal movedSD-lacZ aphA	$\Delta rpsU2$	pKR99
KRLVS112	LVS Tn7::Ptul4-tul4 5'UTR-lacZ aphA	LVS	pKR89
KRLVS111	LVS $\Delta rpsU2$ Tn7::Ptul4-tul4 5'UTR-lacZ aphA	$\Delta rpsU2$	pKR89
KRLVS158	LVS Tn7::Ptul4-pdpA 5'UTR-idealSD-lacZ aphA	LVS	pKR129
KRLVS160	LVS $\Delta rpsU2$ Tn7::Ptul4-pdpA 5'UTR-idealSD-lacZ aphA	$\Delta rpsU2$	pKR129
KRLVS159	LVS Tn7::Ptul4-pdpA 5'UTR-tul4SD-lacZ aphA	LVS	pKR130
KRLVS161	LVS $\Delta rpsU2$ Tn7::Ptul4-pdpA 5'UTR-tul4SD-lacZ aphA	$\Delta rpsU2$	pKR130
KRLVS266	LVS Tn7::Ptul4-pdpA 5'UTR-lacZ aphA pF-nat	KRLVS96	pF-nat
KRLVS267	LVS $\Delta rpsU2$ Tn7::Ptul4-pdpA 5'UTR-lacZ aphA pF-nat	KRLVS97	pF-nat
KRLVS268	LVS $\Delta rpsU2$ Tn7::Ptul4-pdpA 5'UTR-lacZ aphA pF-nat-rpsU2-V	KRLVS97	pKR15
KRLVS269	LVS Tn7::Ptul4-tul4 5'UTR-lacZ aphA pF-nat	KRLVS112	pF-nat
KRLVS270	LVS $\Delta rpsU2$ Tn7::Ptul4-tul4 5'UTR-lacZ aphA pF-nat	KRLVS111	pF-nat
pF-GFP reporter strains			
KRLVS180	LVS pF-tul4UTR-GFP	LVS	pKR145
KRLVS182	LVS $\Delta rpsU2$ pF-tul4UTR-GFP	$\Delta rpsU2$	pKR145
KRLVS234	LVS Δhfq pF-tul4 UTR-GFP	Δhfq	pKR145
KRLVS181	LVS pF-pdpAUTR-GFP	LVS	pKR146
KRLVS183	LVS $\Delta rpsU2$ pF-pdpAUTR-GFP	$\Delta rpsU2$	pKR146
KRLVS236	LVS Δhfq pF-pdpA UTR-GFP	Δhfq	pKR146
KRLVS188	LVS pF-mraYUTR-GFP	LVS	pKR151
KRLVS189	LVS $\Delta rpsU2$ pF-mraYUTR-GFP	$\Delta rpsU2$	pKR151
KRLVS190	LVS pF-FTL_0215UTR-GFP	LVS	pKR152
KRLVS191	LVS $\Delta rpsU2$ pF-FTL_0215UTR-GFP	$\Delta rpsU2$	pKR152
KRLVS199	LVS pF-mraYUTR_mut1-GFP	LVS	pKR156
KRLVS200	LVS $\Delta rpsU2$ pF-mraYUTR_mut1-GFP	$\Delta rpsU2$	pKR156
KRLVS201	LVS pF-mraYUTR_mut2-GFP	LVS	pKR157
KRLVS202	LVS $\Delta rpsU2$ pF-mraYUTR_mut2-GFP	$\Delta rpsU2$	pKR157
KRLVS206	LVS pF-iglAUTR-GFP	LVS	pKR160
KRLVS207	LVS $\Delta rpsU2$ pF-iglAUTR-GFP	$\Delta rpsU2$	pKR160
KRLVS208	LVS pF-FTL_0222UTR-GFP	LVS	pKR161
KRLVS209	LVS $\Delta rpsU2$ pF-FTL_0222UTR-GFP	$\Delta rpsU2$	pKR161
KRLVS210	LVS pF-FTL_0881UTR-GFP	LVS	pKR162
KRLVS211	LVS $\Delta rpsU2$ pF-FTL_0881UTR-GFP	$\Delta rpsU2$	pKR162
KRLVS212	LVS pF-FTL_1093UTR-GFP	LVS	pKR163
KRLVS213	LVS $\Delta rpsU2$ pF-FTL_1093UTR-GFP	$\Delta rpsU2$	pKR163
KRLVS214	LVS pF-mraYUTR_mut5-GFP	LVS	pKR165
KRLVS215	LVS $\Delta rpsU2$ pF-mraYUTR_mut5-GFP	$\Delta rpsU2$	pKR165
KRLVS222	LVS pF-mraYUTR_idealSD-GFP	LVS	pKR169
KRLVS223	LVS $\Delta rpsU2$ pF-mraYUTR_idealSD-GFP	$\Delta rpsU2$	pKR169
KRLVS228	LVS pF-hfqUTR-GFP	LVS	pKR172
KRLVS229	LVS $\Delta rpsU2$ pF-hfqUTR-GFP	$\Delta rpsU2$	pKR172
KRLVS243	LVS pF-mraYUTR_mut6-GFP	LVS	pKR175
KRLVS244	LVS $\Delta rpsU2$ pF-mraYUTR_mut6-GFP	$\Delta rpsU2$	pKR175
KRLVS247	LVS pF-mraYUTR_mut7-GFP	LVS	pKR177
KRLVS248	LVS $\Delta rpsU2$ pF-mraYUTR_mut7-GFP	$\Delta rpsU2$	pKR177

Strain Number	Description	Genetic Background	Plasmid
KRLVS252	LVS pF- <i>mra</i> YUTR_mut8-GFP	LVS	pKR179
KRLVS253	LVS $\Delta rpsU2$ pF- <i>mra</i> YUTR_mut8-GFP	$\Delta rpsU2$	pKR179
KRLVS260	LVS pF- <i>mra</i> YUTR_mut9-GFP	LVS	pKR180
KRLVS261	LVS $\Delta rpsU2$ pF- <i>mra</i> YUTR_mut9-GFP	$\Delta rpsU2$	pKR180
KRLVS262	LVS pF- <i>mra</i> YUTR_mut3-GFP	LVS	pKR182
KRLVS263	LVS $\Delta rpsU2$ pF- <i>mra</i> YUTR_mut3-GFP	$\Delta rpsU2$	pKR182
KRLVS264	LVS pF- <i>mra</i> YUTR_mut4-GFP	LVS	pKR183
KRLVS265	LVS $\Delta rpsU2$ pF- <i>mra</i> YUTR_mut4-GFP	$\Delta rpsU2$	pKR183
Deletion strains			
KMLFT97	LVS Δhfq	LVS	pKL111
VSV-G tagged strains			
KRLVS194	LVS <i>hfq</i> -VSVG	LVS	pKR158
KRLVS195	LVS $\Delta rpsU2$ <i>hfq</i> -VSVG	$\Delta rpsU2$	pKR158

β -galactosidase assays

β -galactosidase assays using *F. tularensis* LVS or $\Delta rpsU2$ cells containing indicated reporter constructs were conducted as previously described (Charity et al., 2009). If significant yellow color was not produced within two hours, reactions were stopped at 120 minutes. Experiments were conducted at least twice in biological triplicate.

GFP assays

F. tularensis LVS, $\Delta rpsU2$, or Δhfq reporter constructs were grown in sMHB to mid-log phase in biological triplicate. Cells were pelleted and resuspended in PBS. A_{600} and fluorescence with excitation of 495 nm and emission of 535 nm were determined using ID3 plate reader (RI-INBRE CRCF), in technical triplicate. Fluorescence readings were normalized to A_{600} and fluorescence of LVS cells (lacking any GFP reporter) was subtracted from each reading to account for basal level fluorescence of the cells. Experiments were conducted at least twice in biological triplicate.

Plasmid copy number qPCR

Wild-type LVS or LVS $\Delta rpsU2$ cells with pF plasmids were grown to mid-log ($OD_{600} = 0.3$ - 0.4). Total DNA was extracted from 1 mL culture using the MasterPure Complete DNA

501 purification kit (Lucigen). qRT-PCR was performed using PowerUp SYBR Green Master Mix
502 (Applied Biosystems) and a Roche LightCycler 480 (RI-INBRE CRCF) essentially as described
503 (Charity et al., 2007) with 0.05 ng of DNA. DNA abundances were calculated for an opening
504 reading frame (ORF3) on the plasmid and relative abundance is reported compared to a
505 chromosomally-encoded control gene, *tul4*. Experiments comparing wild-type and *rpsU2* mutant
506 cells were performed three times in biological triplicate.

507 **5' UTR secondary structure prediction**

508 Secondary structures reported above were predicted using the MXfold2 web server (Sato
509 et al., 2021).

510 **5' UTR motif analyses**

511 The 5' UTRs of genes that have decreases in protein, but not transcript, abundance in
512 cells lacking bS21-2 compared to wild-type (Trautmann & Ramsey, 2022) were analyzed. As
513 there is insufficient annotation of transcriptional start sites in *F. tularensis* LVS, 100 nucleotides
514 upstream of the start codon along with the first six codons were chosen for analysis.

515 STREME software (MEME suite) was used to analyze the 5' UTRs of the 20 genes with
516 the largest fold decreases in protein in $\Delta rpsU2$ cells compared to LVS. These were compared
517 to shuffled sequences to find two candidate motifs. As a control, the same parameters were
518 used to compare the predicted 5' UTRs of 20 genes not differentially expressed in LVS and
519 $\Delta rpsU2$.

520 Shine-Dalgarno predictions were made by highest similarity to the reverse complement
521 of the anti-Shine-Dalgarno (5'-AGGAGG-3') within 20 nucleotides of the start codon.

522 **Immunoblotting**

Immunoblotting was completed as previously described (Trautmann & Ramsey, 2022). Briefly, cell lysates were separated by SDS-PAGE, transferred to PVDF, and analyzed for total protein with the Invitrogen No-Stain Protein labeling reagent for normalization. Membranes were probed with indicated monoclonal antibodies (BEI Resources, diluted 1:250 for PdpB, 1:1000 for IgIB, and 1:1000 for IgIA) or the VSV-G epitope tag (Sigma, diluted 1:2222) in blocking buffer. Proteins were detected using IRDye 800 CW donkey anti-mouse IgG or donkey anti-rabbit IgG secondary antibodies (Li-Cor, diluted 1:10,000). Protein abundance was calculated as fluorescence of protein bands relative to total protein in each lane. Experiments were performed at least twice in biological triplicate.

RNA purification and qRT-PCR

Total RNA was purified according to the RNAsnapTM protocol (Stead et al., 2012). *F. tularensis* LVS was grown in biological triplicate to mid-log phase. Pelleted cells (10 mL) were resuspended in 100 µl of fresh RES (95% formamide, 18 mM EDTA, 0.025% SDS, 1% BME), then incubated at 95°C for 7 minutes. Cell debris were pelleted by centrifugation and the supernatant was preserved. Total nucleic acid was recovered with 0.3M sodium acetate (pH 5.2) and 3x volumes 100% ethanol. Samples were stored at -80°C for 1 hour, then nucleic acid was pelleted by centrifugation at 4°C for 30 minutes. The pellet was washed with 75% ethanol and resuspended in water. Purified nucleic acids were treated with RQ1 DNase (Promega) for 1 hour at 37°C and RNA was purified again with sodium acetate/ethanol precipitation.

cDNA was synthesized using Superscript III reverse transcriptase (Life Technologies) as previously described (Charity et al., 2007). qRT-PCR was performed with the PowerUP SYBR Green Master Mix (Applied Biosystems) and the Roche Lightcycler 480 (RI-INBRE CRCF).

545 Transcript abundances of *pdpA*, *pdpB*, *iglA*, *pigR*, *rpoA1*, and *bfr* were normalized to a control
546 gene, *tul4*. Experiments were conducted twice in biological triplicate.

547

548 **Acknowledgements**

549 We thank the other members of the Ramsey laboratory for support and helpful
550 discussions and Dr. Simon Dove for his helpful comments on the manuscript and his support of
551 KMR as a post-doctoral fellow when she constructed the *F. tularensis* Δhfq strain. We also thank
552 Janet Atoyan and the Rhode Island INBRE Molecular Informatics Core.

553

554 **Funding Information**

555 This work was funded by an NIGMS CARTD-COBRE Pilot Project Award
556 (P20GM121344-KMR), an NIGMS/RI-INBRE Early Career Development Award
557 (P20GM103430-KMR), and a Rhode Island Foundation Medical Research Grant
558 (2798_20190602-KMR). This work was supported by the USDA National Institute of Food and
559 Agriculture, Hatch Formula project accession number 1017848. This material is based upon
560 work conducted at a Rhode Island NSF EPSCoR research facility, the Genomics and
561 Sequencing Center, supported in part by the National Science Foundation EPSCoR Cooperative
562 Agreements 0554548, EPS-1004057, and OIA-1655221. The research was made possible using
563 equipment and services available through the Rhode Island Institutional Development Award
564 (IDeA) Network of Biomedical Research Excellence from the National Institute of General
565 Medical Sciences of the National Institutes of Health under grant number P20GM103430 through
566 the Centralized Research Core facility and the Molecular Informatics Core (RRID:SCR_017685).

567 Antibodies for the following *Francisella tularensis* proteins were obtained through BEI
568 Resources, NIAID, NIH: PdpB, IgIA, and IgIB.

569

570 **References**

- 571 Bailey, T. L. (2021). *STREME: accurate and versatile sequence motif discovery* [Bioinformatics].
- 572 Bubunencko, M., Baker, T. & Court, D. L. (2007). Essentiality of ribosomal and transcription
573 antitermination proteins analyzed by systematic gene replacement in *Escherichia coli*.
574 *Journal of Bacteriology*, 189(7), 2844-2853. <https://doi.org/10.1128/JB.01713-06>.
- 575 Byrgazov, K., Vesper, O., & Moll, I. (2013). Ribosome heterogeneity: Another level of complexity
576 in bacterial translation regulation. *Current Opinion in Microbiology*, 16(2), 133–139.
577 <https://doi.org/10.1016/j.mib.2013.01.009>
- 578 Chambers, J. R., & Bender, K. S. (2011). The RNA Chaperone Hfq Is Important for Growth and
579 Stress Tolerance in *Francisella novicida*. *PLoS ONE*, 6(5), e19797.
580 <https://doi.org/10.1371/journal.pone.0019797>
- 581 Chang, C., & Craven, G. R. (1977). Identification of several proteins involved in the messenger
582 RNA binding site of the 30 S ribosome by inactivation with 2-methoxy-5-nitrotrypone.
583 *Journal of Molecular Biology*, 117(2), 401–418. [https://doi.org/10.1016/0022-](https://doi.org/10.1016/0022-2836(77)90135-8)
584 [2836\(77\)90135-8](https://doi.org/10.1016/0022-2836(77)90135-8)
- 585 Charity, J. C., Blalock, L. T., Costante-Hamm, M. M., Kasper, D. L., & Dove, S. L. (2009). Small
586 Molecule Control of Virulence Gene Expression in *Francisella tularensis*. *PLOS*
587 *Pathogens*, 5(10), e1000641. <https://doi.org/10.1371/journal.ppat.1000641>
- 588 Charity, J. C., Costante-Hamm, M. M., Balon, E. L., Boyd, D. H., Rubin, E. J., & Dove, S. L.
589 (2007). Twin RNA Polymerase–Associated Proteins Control Virulence Gene Expression
590 in *Francisella tularensis*. *PLoS Pathogens*, 3(6), e84.
591 <https://doi.org/10.1371/journal.ppat.0030084>
- 592 Chen, L.-X., Jaffe, A. L., Borges, A. L., Penev, P. I., Nelson, T. C., Warren, L. A., & Banfield, J.
593 F. (2022). Phage-encoded ribosomal protein S21 expression is linked to late-stage phage
594 replication. *ISME Communications*, 2(1), Article 1. [https://doi.org/10.1038/s43705-022-](https://doi.org/10.1038/s43705-022-00111-w)
595 [00111-w](https://doi.org/10.1038/s43705-022-00111-w)
- 596 de Smit, M. H., & van Duin, J. (1994). Control of translation by mRNA secondary structure in
597 *Escherichia coli*. A quantitative analysis of literature data. *Journal of Molecular Biology*,
598 244(2), 144–150. <https://doi.org/10.1006/jmbi.1994.1714>
- 599 Ferretti, M. B., & Karbstein, K. (2019). Does functional specialization of ribosomes really exist?
600 *RNA*, 25(5), 521–538. <https://doi.org/10.1261/rna.069823.118>
- 601 Fu, L., Cao, Y., Wu, J., Peng, Q., Nie, Q., & Xie, X. (2022). UFold: Fast and accurate RNA
602 secondary structure prediction with deep learning. *Nucleic Acids Research*, 50(3), e14.
603 <https://doi.org/10.1093/nar/gkab1074>

604 Genuth, N. R., & Barna, M. (2018). The Discovery of Ribosome Heterogeneity and Its
605 Implications for Gene Regulation and Organismal Life. *Molecular Cell*, 71(3), 364–374.
606 <https://doi.org/10.1016/j.molcel.2018.07.018>

607 Hall, M. N., Gabay, J., Débarbouillé, M., & Schwartz, M. (1982). A role for mRNA secondary
608 structure in the control of translation initiation. *Nature*, 295(5850), 616–618.
609 <https://doi.org/10.1038/295616a0>

610 Held, W. A., Nomura, M., Hershey, J. W. (1974). Ribosomal protein S21 is required for full activity
611 in the initiation of protein synthesis. *Molecular and General Genetics* 128(1):11-22.
612 <https://doi.org/10.1007/BF00267291>.

613 Jha, V., Roy, B., Jahagirdar, D., McNutt, Z. A., Shatoff, E. A., Boleratz, B. L., Watkins, D. E.,
614 Bundschuh, R., Basu, K., Ortega, J., & Fredrick, K. (2020). Structural basis of
615 sequestration of the anti-Shine-Dalgarno sequence in the Bacteroidetes ribosome.
616 *Nucleic Acids Research*, 49(1), 547–567. <https://doi.org/10.1093/nar/gkaa1195>

617 Kaledhonkar, S., Fu, Z., Caban, K., Li, W., Chen, B., Sun, M., Gonzalez, R. L., & Frank, J. (2019).
618 Late steps in bacterial translation initiation visualized using time-resolved cryo-EM.
619 *Nature*, 570(7761), Article 7761. <https://doi.org/10.1038/s41586-019-1249-5>

620 Lenco, J., Tambor, V., Link, M., Klimentova, J., Dresler, J., Peterek, M., Charbit, A., & Stulik, J.
621 (2014). Changes in proteome of the Δhfq strain derived from *Francisella tularensis* LVS
622 correspond with its attenuated phenotype. *PROTEOMICS*, 14(21–22), 2400–2409.
623 <https://doi.org/10.1002/pmic.201400198>

624 Link, T. M., Valentin-Hansen, P., & Brennan, R. G. (2009). Structure of Escherichia coli Hfq
625 bound to polyriboadenylate RNA. *Proceedings of the National Academy of Sciences*,
626 106(46), 19292–19297. <https://doi.org/10.1073/pnas.0908744106>

627 Lorenz, R., Bernhart, S. H., Höner zu Siederdissen, C., Tafer, H., Flamm, C., Stadler, P. F., &
628 Hofacker, I. L. (2011). ViennaRNA Package 2.0. *Algorithms for Molecular Biology*, 6(1),
629 26. <https://doi.org/10.1186/1748-7188-6-26>

630 LoVullo, E. D., Molins-Schneekloth, C. R., Schweizer, H. P., & Pavelka, M. S. (2009). Single-
631 copy chromosomal integration systems for *Francisella tularensis*. *Microbiology*, 155(Pt 4),
632 1152–1163. <https://doi.org/10.1099/mic.0.022491-0>

633 Maier, T. M., Havig, A., Casey, M., Nano, F. E., Frank, D. W., & Zahrt, T. C. (2004). Construction
634 and Characterization of a Highly Efficient Francisella Shuttle Plasmid. *Applied and*
635 *Environmental Microbiology*, 70(12), 7511–7519.
636 <https://doi.org/10.1128/AEM.70.12.7511-7519.2004>

637 McNutt, Z. A., Roy, B., Gemler, B. T., Shatoff, E. A., Moon, K.-M., Foster, L. J., Bundschuh, R.,
638 & Fredrick, K. (2023). Ribosomes lacking bS21 gain function to regulate protein synthesis
639 in *Flavobacterium johnsoniae*. *Nucleic Acids Research*, 51(4), 1927-1942.
640 <https://doi.org/10.1093/nar/gkad047>

641 Meibom, K. L., Forslund, A.-L., Kuoppa, K., Alkhuder, K., Dubail, I., Dupuis, M., Forsberg, Å., &
642 Charbit, A. (2009). Hfq, a Novel Pleiotropic Regulator of Virulence-Associated Genes in
643 *Francisella tularensis*. *Infection and Immunity*, 77(5), 1866–1880.
644 <https://doi.org/10.1128/IAI.01496-08>

645 Mizuno, C. M., Guyomar, C., Roux, S., Lavigne, R., Rodriguez-Valera, F., Sullivan, M. B., Gillet,
646 R., Forterre, P., & Krupovic, M. (2019). Numerous cultivated and uncultivated viruses
647 encode ribosomal proteins. *Nature Communications*, 10(1), 752.
648 <https://doi.org/10.1038/s41467-019-08672-6>

649 Mizushima, S., & Nomura, M. (1970). Assembly mapping of 30S ribosomal proteins from *E. coli*.
650 *Nature*, 226(5252), 1214. <https://doi.org/10.1038/2261214a0>

651 Park, H.-S., Östberg, Y., Johansson, J., Wagner, E. G. H., & Uhlin, B. E. (2010). Novel role for
652 a bacterial nucleoid protein in translation of mRNAs with suboptimal ribosome-binding
653 sites. *Genes & Development*, 24(13), 1345–1350. <https://doi.org/10.1101/gad.576310>

654 Postic, G., Dubail, I., Frapy, E., Dupuis, M., Dieppedale, J., Charbit, A., & Meibom, K. L. (2012).
655 Identification of a Novel Small RNA Modulating *Francisella tularensis* Pathogenicity. *PLoS*
656 *ONE*, 7(7), e41999. <https://doi.org/10.1371/journal.pone.0041999>

657 Postic, G., Frapy, E., Dupuis, M., Dubail, I., Livny, J., Charbit, A., & Meibom, K. L. (2010).
658 Identification of small RNAs in *Francisella tularensis*. *BMC Genomics*, 11, 625.
659 <https://doi.org/10.1186/1471-2164-11-625>

660 Ramsey, K. M., Ledvina, H. E., Tresko, T. M., Wandzilak, J. M., Tower, C. A., Tallo, T., Schramm,
661 C. E., Peterson, S. B., Skerrett, S. J., Mougous, J. D., & Dove, S. L. (2020). Tn-Seq
662 reveals hidden complexity in the utilization of host-derived glutathione in *Francisella*
663 *tularensis*. *PLOS Pathogens*, 16(6), e1008566.
664 <https://doi.org/10.1371/journal.ppat.1008566>

665 Ramsey, K. M., Osborne, M. L., Vvedenskaya, I. O., Su, C., Nickels, B. E., & Dove, S. L. (2015).
666 Ubiquitous promoter-localization of essential virulence regulators in *Francisella*
667 *tularensis*. *PLoS Pathogens*, 11(4), e1004793.
668 <https://doi.org/10.1371/journal.ppat.1004793>

669 Robertson, W. R., Dowsett, S. J., & Hardy, S. J. S. (1977). Exchange of ribosomal proteins
670 among the ribosomes of *Escherichia coli*. *Molecular and General Genetics MGG*, 157(2),
671 205–214. <https://doi.org/10.1007/BF00267399>

672 Rohlifing, A. E., Dove, S. L. (2014). Coordinate control of virulence gene expression in *Francisella*
673 *tularensis* involves direct interaction between key regulators. *Journal of Bacteriology*,
674 196(19). <https://doi.org/10.1128/JB.01700-14>.

675 Rohlifing, A. E., Ramsey, K. M., & Dove, S. L. (2018). Polyphosphate Kinase Antagonizes
676 Virulence Gene Expression in *Francisella tularensis*. *Journal of Bacteriology*, 200(3).
677 <https://doi.org/10.1128/JB.00460-17>

- 678 Sato, K., Akiyama, M., & Sakakibara, Y. (2021). RNA secondary structure prediction using deep
679 learning with thermodynamic integration. *Nature Communications*, 12(1), 941.
680 <https://doi.org/10.1038/s41467-021-21194-4>
- 681 Shimojo, M., Amikura, K., Masuda, K., Kanamori, T., Ueda, T., Shimizu, Y. (2020) *In vitro*
682 reconstitution of functional small ribosomal subunit assembly for comprehensive analysis
683 of ribosomal elements in *E. coli*. *Communications Biology*, 3(1), 142.
684 <https://doi.org/10.1038/s42003-020-0874-8>.
- 685 Stead, M. B., Agrawal, A., Bowden, K. E., Nasir, R., Mohanty, B. K., Meagher, R. B., & Kushner,
686 S. R. (2012). RNA snap TM: A rapid, quantitative and inexpensive, method for isolating
687 total RNA from bacteria. *Nucleic Acids Research*, 40(20), e156–e156.
688 <https://doi.org/10.1093/nar/gks680>
- 689 Trautmann, H. S., & Ramsey, K. M. (2022). A Ribosomal Protein Homolog Governs Gene
690 Expression and Virulence in a Bacterial Pathogen. *Journal of Bacteriology*, 204(10),
691 e0026822. <https://doi.org/10.1128/jb.00268-22>
- 692 van Duin, J., & Wijnands, R. (1981). The Function of Ribosomal Protein S21 in Protein Synthesis.
693 *European Journal of Biochemistry*, 118(3), 615–619. [https://doi.org/10.1111/j.1432-](https://doi.org/10.1111/j.1432-1033.1981.tb05563.x)
694 [1033.1981.tb05563.x](https://doi.org/10.1111/j.1432-1033.1981.tb05563.x)
- 695 Watson, Z. L., Ward, F. R., Méheust, R., Ad O., Schepartz, A., Banfield, J. F., & Cate, J. H. D.
696 (2020) Structure of the bacterial ribosome at 2 Å resolution. *Elife*, 9:e60482.
697 <https://doi.org/10.7554/eLife.60482>.

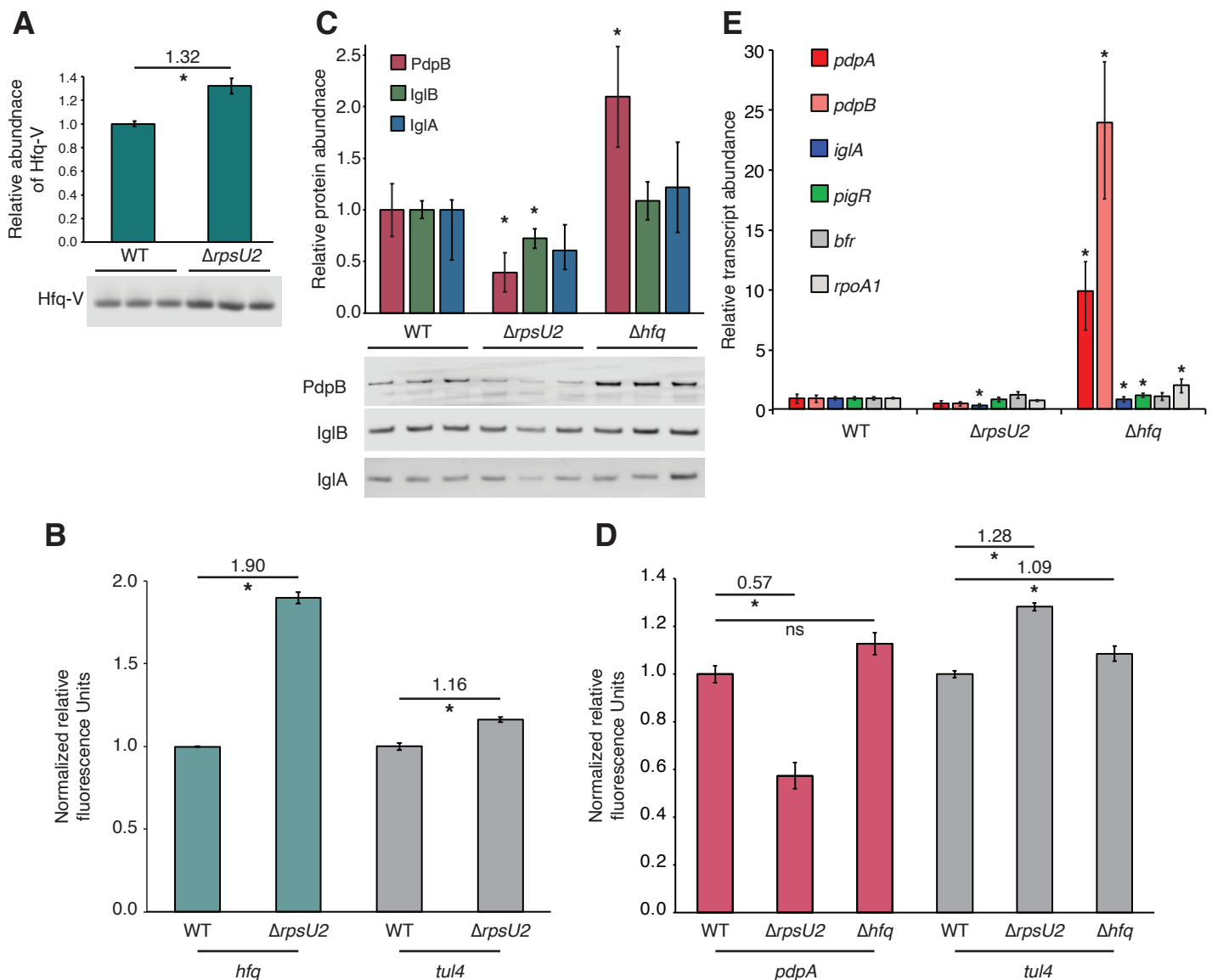


Figure 1. Hfq and bS21-2 influence production of T6SS proteins via different pathways. (A) Cells lacking bS21-2 have more Hfq. Bottom: Immunoblots probed with anti-VSV-G antibody. Whole cell lysates from bacteria containing Hfq-VSV-G and either with (WT) or without ($\Delta rpsU2$) bS21-2, in biological triplicate. Top: Quantification of immunoblots. Band intensities for each protein were normalized to total protein per lane on the membrane. **(B)** Loss of bS21-2 leads to more *hfq* translation. Relative fluorescence is reported for translational fusion reporters containing the 5' UTR of either *hfq* or *tul4* fused to *gfp* in cells with (WT) or without ($\Delta rpsU2$) bS21-2, in biological triplicate. Values relative to WT for each 5' UTR are shown. **(C)** Only some of the T6SS proteins are influenced by loss of Hfq. Bottom: Immunoblots probed with antibodies to indicated T6SS proteins in lysates of WT cells, cells lacking bS21-2 ($\Delta rpsU2$), or cells lacking Hfq (Δhfq). Top: Quantification of immunoblots. Band intensities for each protein were normalized to total protein per lane on the membrane. **(D)** Hfq does not influence translation of the T6SS protein PdpA. Relative fluorescence for translational fusion reporters containing the 5' UTR of either *pdpA* or *tul4* fused to *gfp* in WT cells, cells lacking bS21-2 ($\Delta rpsU2$), or cells lacking Hfq (Δhfq), in biological triplicate. **(E)** Hfq is a negative regulator of T6SS gene transcript abundance. Quantitative real-time PCR was used to determine the relative transcript abundance for indicated FPI-encoded genes in WT cells, cells lacking bS21-2 ($\Delta rpsU2$), or cells lacking Hfq (Δhfq), normalized to the *tul4* gene. The *rpoA1* and *bfr* genes are included as additional negative controls, as their expression is not meaningfully influenced by bS21-2. (A-E) Error bars represent 1 SD. Experiments were repeated at least twice and data from a representative experiment are shown. (A-D) * $p < 0.05$ after Bonferroni correction. (E) * $p < 0.005$ after Bonferroni correction.

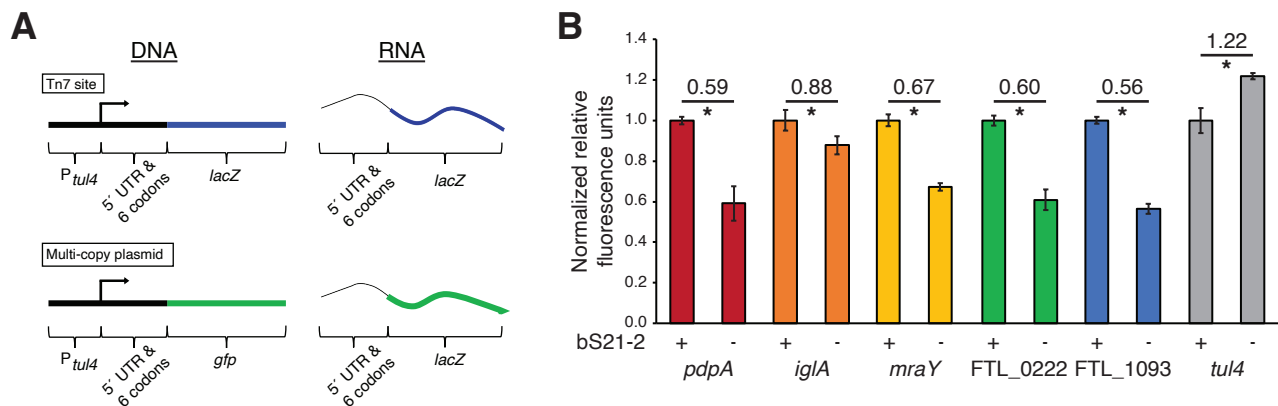


Figure 2. 5' UTRs are sufficient to lead to bS21-2-mediated changes in translation. (A) Diagrams of the translational reporter fusions used. Reporters used the *tul4* promoter to drive expression of the tested 5' UTR, including the first 6 codons of the gene, and are in frame with either *lacZ* at the Tn7 site of the genome or *gfp* on a multi-copy plasmid. **(B)** Relative fluorescence is reported for indicated translational fusion reporters in cells with (+; WT) or without (-; $\Delta rpsU2$) bS21-2 in biological triplicate. The *tul4* reporter serves as a control. 5' UTR sequences can be found in Table 1. Error bars represent 1 SD. * $p < 0.05$ by t-test. Experiments were repeated at least twice and data from a representative experiment are shown.

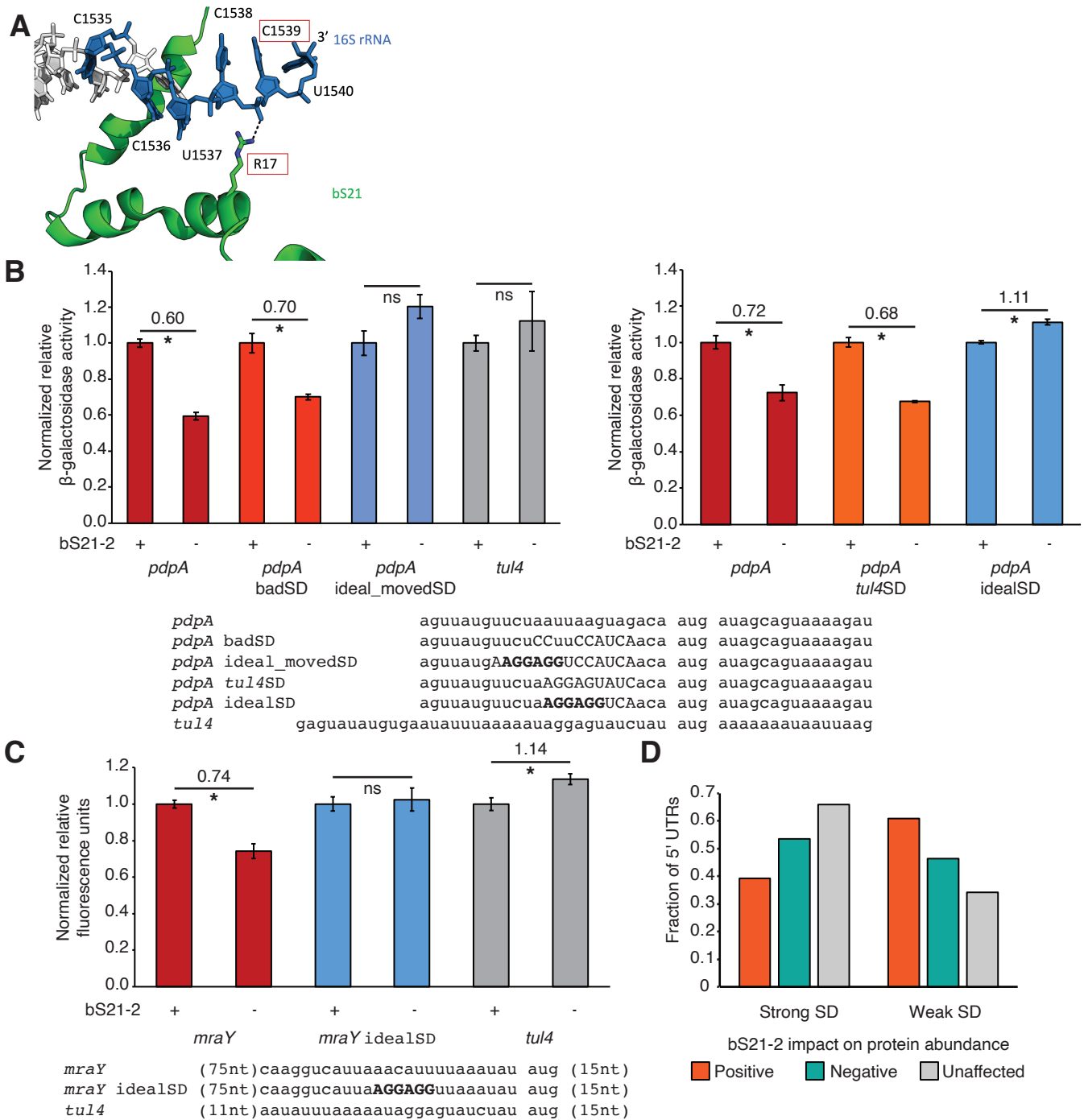
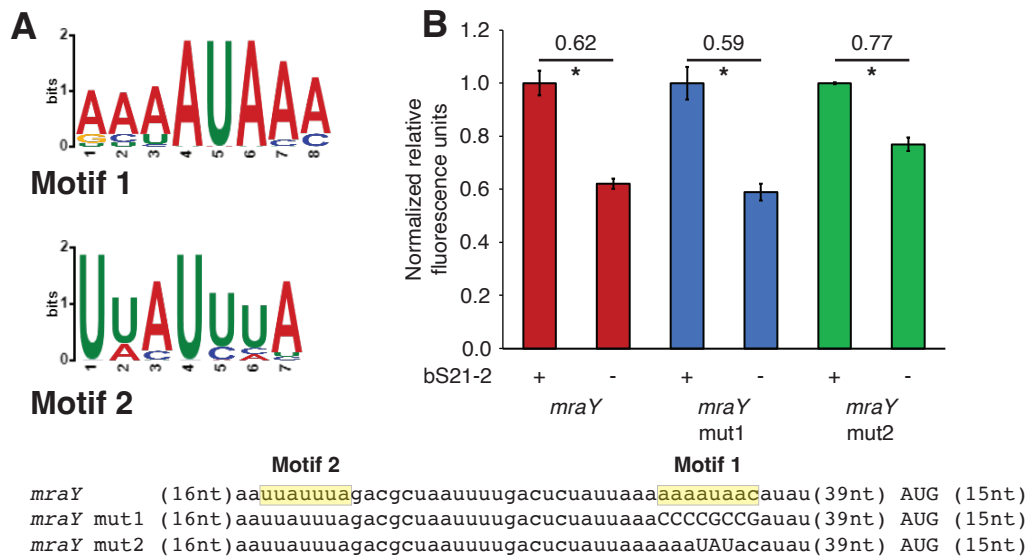


Figure 3. Genes with ideal Shine-Dalgarno (SD) sequences are not responsive to bS21-2. (A) bS21 interacts with the anti-Shine Dalgarno (ASD) sequence. In *E. coli*, amino acid R17 of the sole bS21 protein (green) directly interacts with C1539 of 16S, which is part of the ASD (blue). Measured distance is 2.7Å (PDB 6o7k; Kaledhonkar et al. 2019). (B) Introduction of an ideal SD in the *pdpA* leader leads to loss of bS21-2 responsiveness. Top: Relative β-galactosidase activity from modified or wild-type *pdpA* 5' UTRs in cells with (+; WT) or without (-; Δ*rpsU2*) bS21-2, in biological triplicate. Bottom: Alignment of modifications to *pdpA* 5' UTR. (C) Introduction of an ideal SD in the *mraY* leader leads to loss of bS21-2 responsiveness. Top: Relative fluorescence is reported for indicated translational fusion reporters in cells with (+; WT) or without (-; Δ*rpsU2*) bS21-2, in biological triplicate. Bottom: Alignment of indicated 5' UTRs. (B-C) Value in parenthesis indicates the number of identical nts omitted from 5' end of the UTRs. Capital letters: altered from WT; bold: ideal SD sequences. Error bars represent 1 SD. **p*<0.05 by t-test. ns = not significant. Experiments were repeated at least twice and data from a representative experiment are shown. (D) The absence of strong SD-ASD interactions is correlated with bS21-2 influencing translation. Fraction of genes that are positively-impacted (n=74), negatively-impacted (n=84), or unaffected (n=82) by bS21-2, categorized by strength of SD. "Strong" SD: 4 or more nts complementary to ASD; "weak" SD: 3 or fewer complementary nts.



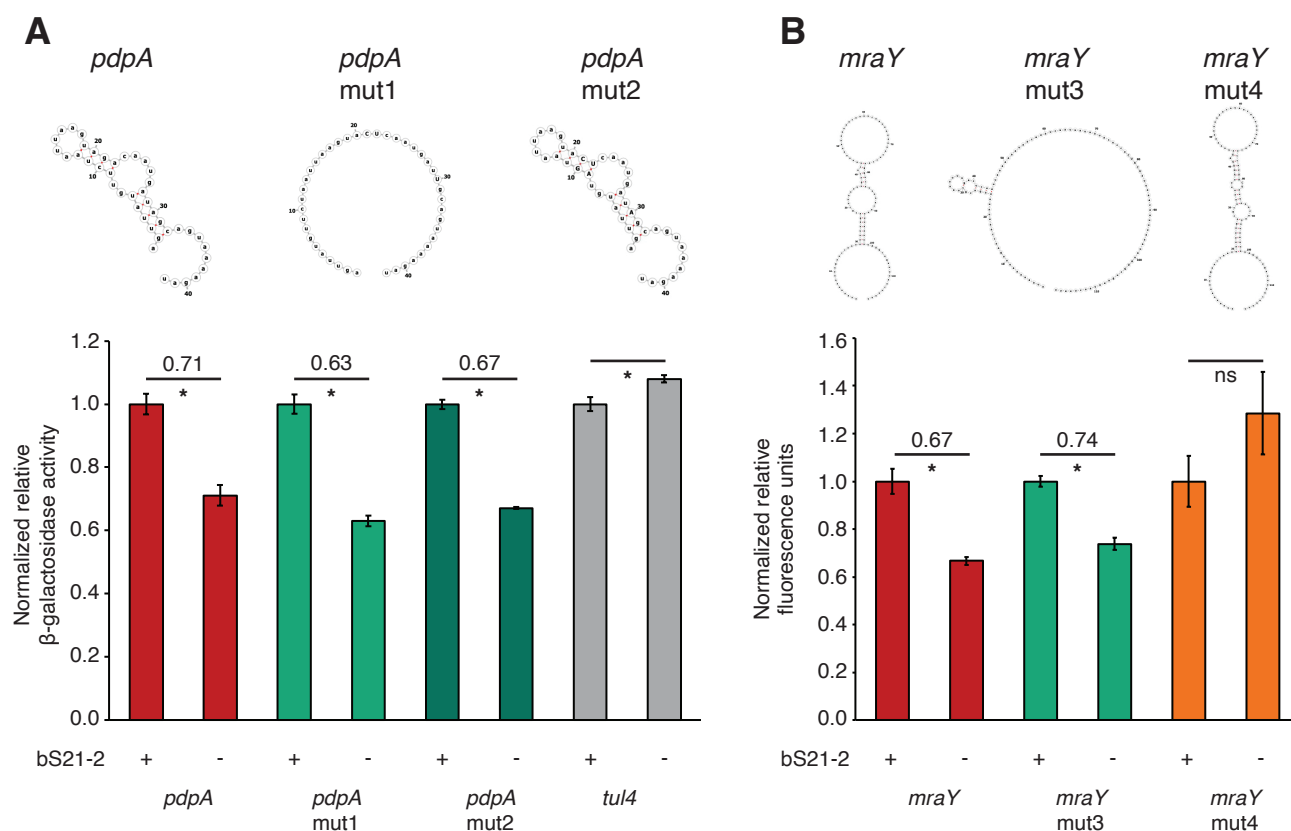


Figure 5. Predicted secondary structure plays no clear role in bS21-2- responsive translation.

(A) Changing the *pdpA* secondary structure does not impact responsiveness to bS21-2. Top: Predicted secondary structures for wild-type and modified *pdpA* 5' UTRs, from MXFold2. Sequence modifications in Table 1. Bottom: Relative β -galactosidase activity from indicated 5' UTR fused to *lacZ*, in cells with (+; WT) or without (-; $\Delta rpsU2$) bS21-2, in biological triplicate. *tul4* is included as a control.

(B) Changing the *mraY* secondary structure does not impact responsiveness to bS21-2. Top: Secondary structure predictions of wild-type and modified *mraY* 5' UTRs, from MXFold2. Sequence modifications in Table 1. Bottom: Relative fluorescence is reported for indicated translational fusion reporters in cells with (+; WT) or without (-; $\Delta rpsU2$) bS21-2, in biological triplicate. (A-B) Error bars represent 1 SD. * $p < 0.05$ by t-test. Experiments were repeated twice and data from a representative experiment are shown.

